

Supporting Information

Crafting "Brick-Mud" Segregated Nanocomposites: A Novel Approach to Superior Electromagnetic Interference Shielding, Electrical Insulation, and Thermal Conductivity in Biopolymers

Tong Liu^{a‡}, Huiyao Feng^{a‡}, Linbing Deng^{a‡}, Chenhong Jin^a, Henri Vahabi^b, Mohammad Reza Saeb^c, Tairong Kuang^{a}*

^a Functional Polymers & Advanced Materials (FPAM) Lab, College of Materials Science and Engineering, Zhejiang University of Technology, Hangzhou 310014, P. R. China

^b Université de Lorraine, CentraleSupélec, LMOPS, Metz, France.

^c Department of Pharmaceutical Chemistry, Medical University of Gdańsk, J. Hallera 107, 80-416 Gdańsk, Poland

[‡]These authors contributed equal to this work.

^{*}*Corresponding author:* T. R. Kuang (E-mail: kuangtr@zjut.edu.cn).

Experimental section

Differential scanning calorimetry (DSC) analysis.

The melting points of PCL/BN and PLA/CNTs composites were characterized by DSC analysis. DSC analyses were conducted with a Q2000TA instrument (Delaware, USA) in a nitrogen atmosphere at a flow rate of 50 mL/min. The analysis of PLA/CNTs composites was carried out in three steps: initial heating from 25 °C to 200 °C, cooling back to 25 °C after a 2 min hold, followed by a second heating from 25 °C to 200 °C. A sample size of 5 mg was used, with both heating and cooling rates set at 10 °C/min. The analysis of PCL/BN composites is the same as above, but the maximum temperature is set to 100°C.

Morphological characterization.

The morphology of the fracture surface for s-xByC and r-xByC composites was observed using a Digital Microscope (DM, DM4, China). The fracture morphology of PLA/CNTs composites was observed using a scanning electron microscope (SEM, Regulus 8100, HITACHI). Before SEM analysis, the fracture surfaces were gold-plated for 90 s in vacuum conditions. The operating voltage for SEM was set at 10 kV. The brittle fracture of the sample was obtained by cooling the sample with liquid nitrogen for 2 h and then rapidly cracking it with force.

Rheological properties measurement.

Rheological properties of the PLA/CNTs composites, with dimensions of 25 mm in diameter and 1 mm in thickness, were assessed using a MCR302 rheometer (Anton Paar, Austria). Analysis was conducted at 180 °C, employing a frequency sweep from 100 to 0.1 rad/s at a constant amplitude of 1 % to guarantee the identification of the linear viscoelastic (LVE) region.

Electrical conductivity measurements.

Electrical conductivity measurements for PLA/CNTs composites were conducted in dry air at ambient temperature using a four-point probe resistivity system (RTS-9, Guangzhou Four Probes Technology Company Ltd., China) and a high-resistance meter (ZC36, Shanghai Anbiao Electronic Co., Ltd., China).

Electromagnetic interference (EMI) shielding performance measurements.

The EMI performance of the 3mm PLA/CNTs composites was evaluated within the X-band frequency range (8.2-12.4 GHz) via a vector network analyzer (Ceyear 3672C-S, Ceyear Technologies Co., Ltd., China). The EMI shielding performance of the material is quantified by the shielding efficiency (SE), which consists of absorption (SE_A), reflection (SE_R), and multiple internal reflections (SE_M). When the total SE (SE_T) exceeds 15 dB, the effect of SE_M becomes negligible. The relevant calculation equations are provided in formulas (1)-(6)[1].

$$T = |S_{12}|^2 = |S_{21}|^2 \#(1)$$

$$R = |S_{11}|^2 = |S_{22}|^2 \#(2)$$

$$A = 1 - T - R \#(3)$$

$$SE_A = -10 \log\left(\frac{T}{1-R}\right) \#(4)$$

$$SE_A = -10 \log(1-R) \#(5)$$

$$SE_T = SE_R + SE_A \#(6)$$

Here, T, R, and A represent the transmission, reflection, and absorption coefficients, respectively. The S-parameters (S_{11} , S_{12} , S_{22} , and S_{21}) were measured using a vector network analyzer.

Supplementary Figures and Tables

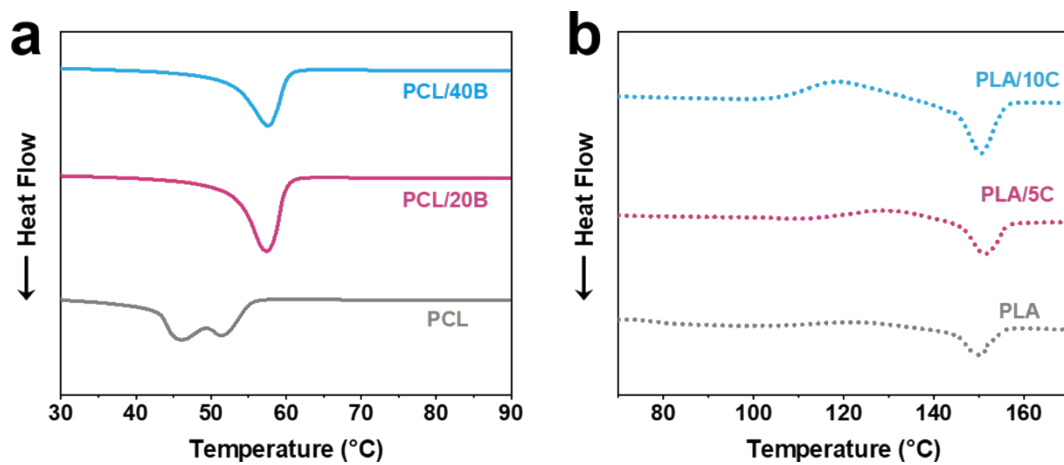


Fig. S1. The second-heating curves of (a) PCL, PCL/20B and PCL/40B and (b) PLA, PLA/5C and PLA/10C.

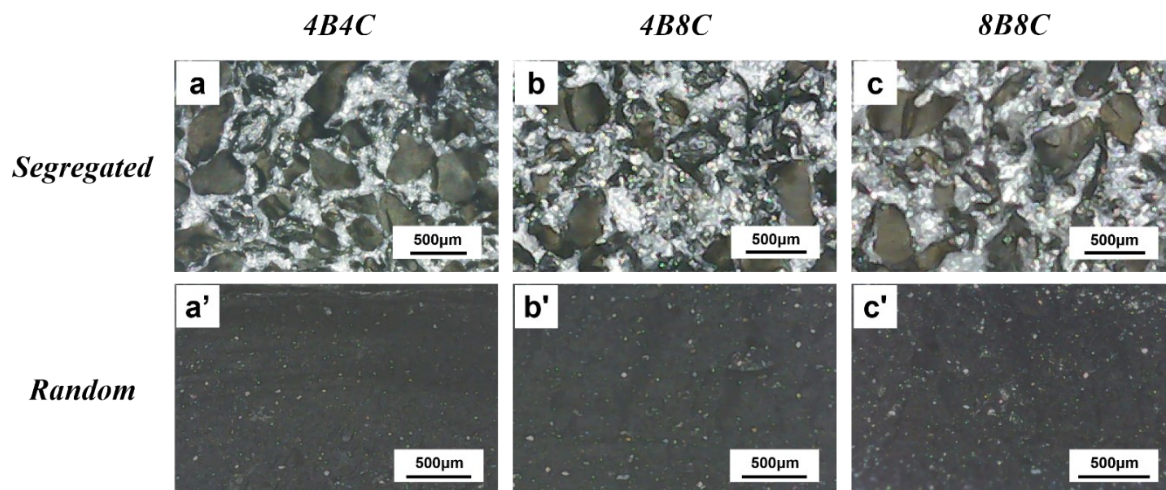


Fig. S2. Digital Microscope images of cryo-fractured surfaces: (a) s-4B4C, (b) s-4B8C, (c) s-8B8C, (a') r-4B4C, (b') r-4B8C, (c') r-8B8C.

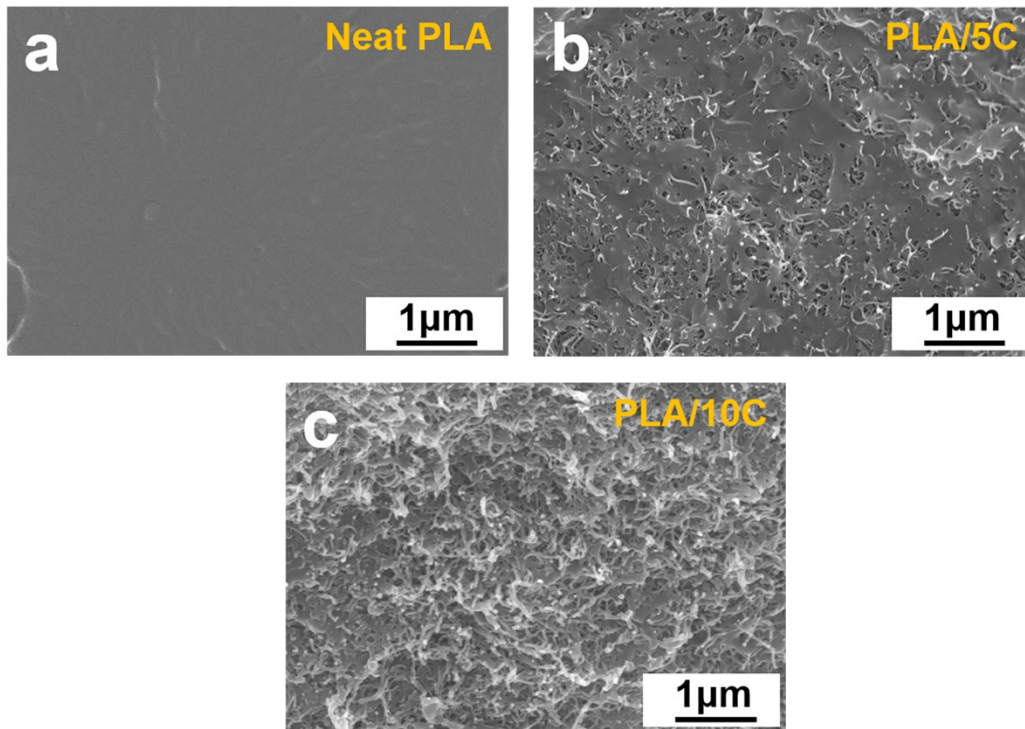


Fig. S3. SEM images of cryo-fractured surfaces: (a)PLA, (b) PLA/5C, (c) PLA/10C.

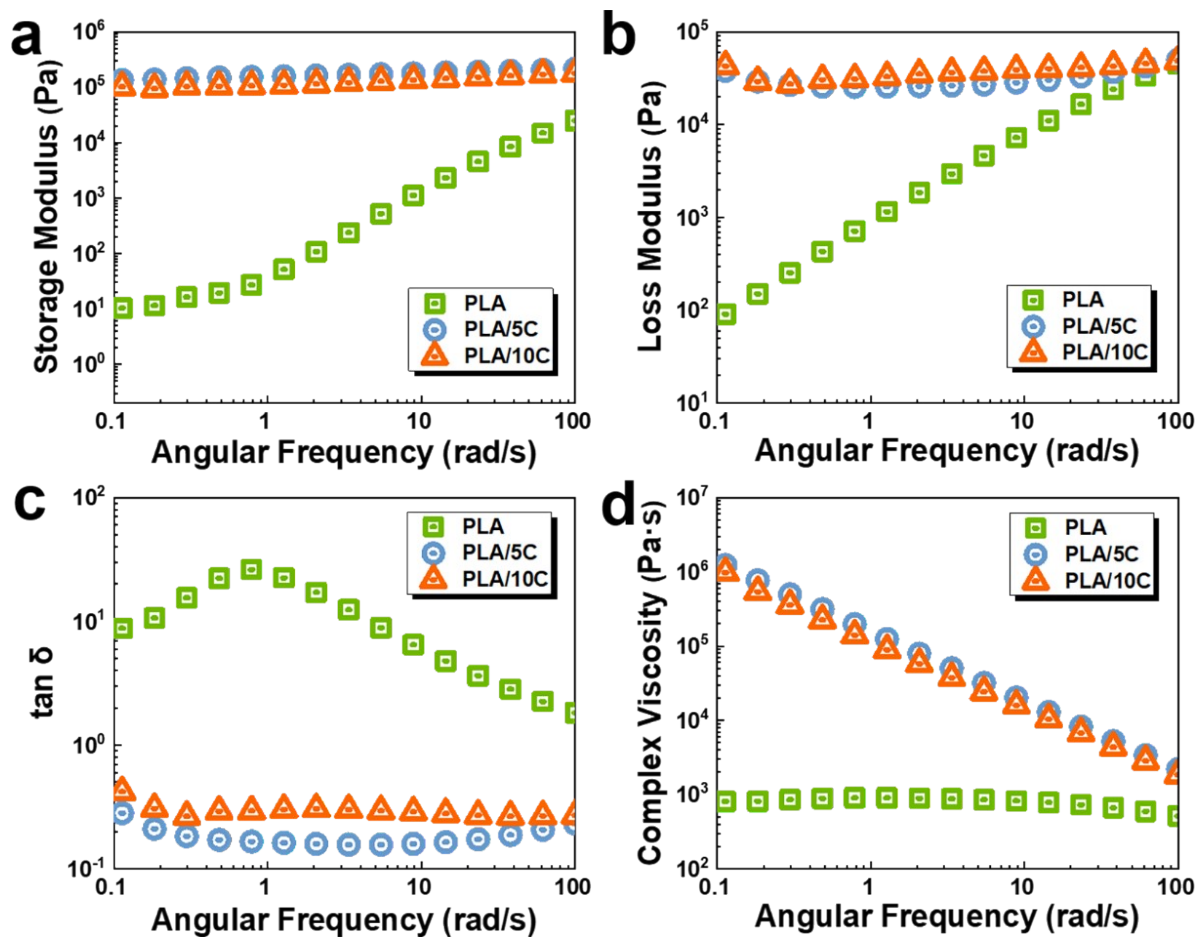


Fig. S4. Rheological properties of PLA and PLA/CNTs composites: (a) storage modulus, (b) loss modulus, (c) $\tan \delta$, (d) complex viscosity.

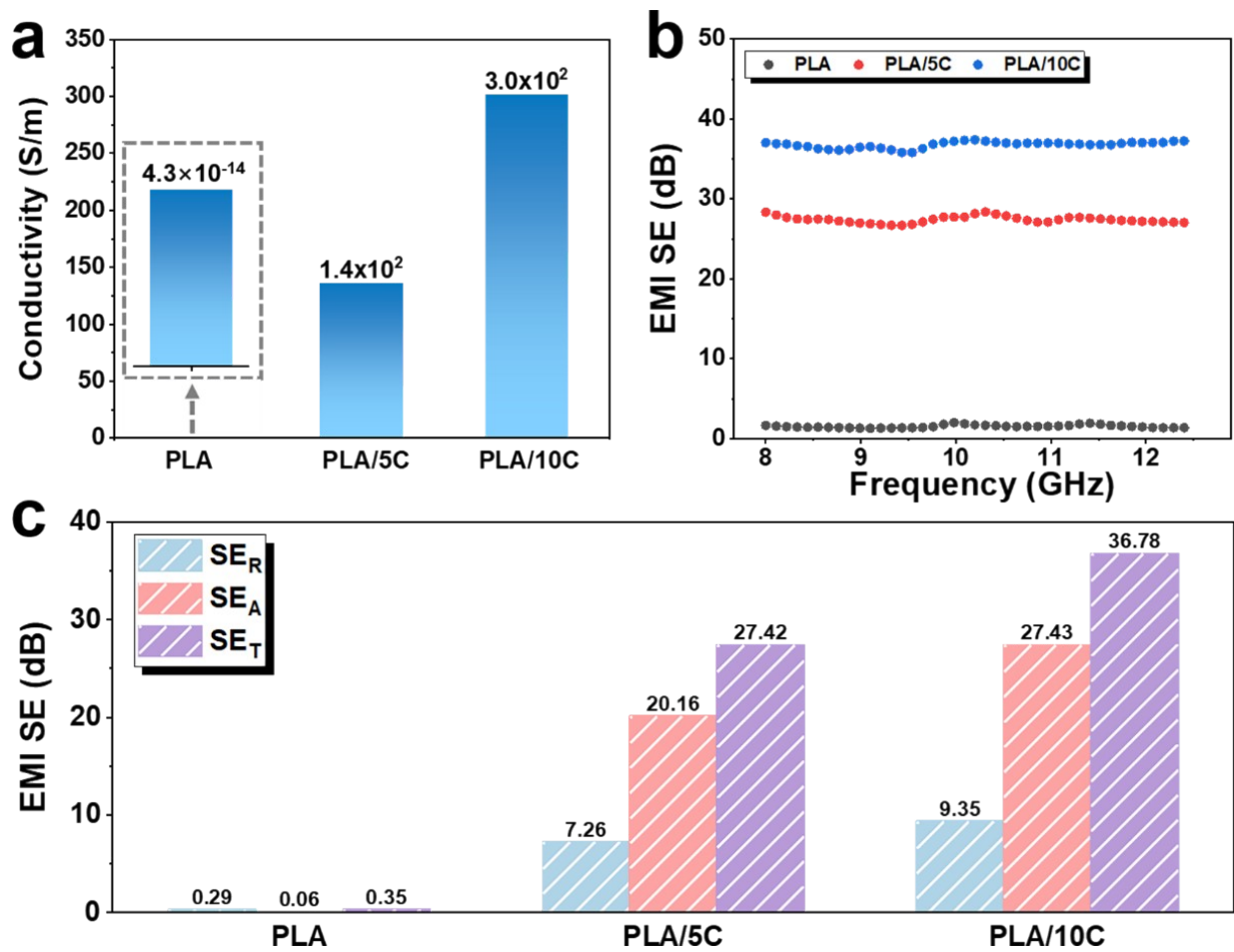


Fig. S5. (a) Electrical conductivity and (b, c) EMI shielding performance of PLA and PLA/CNTs composites.

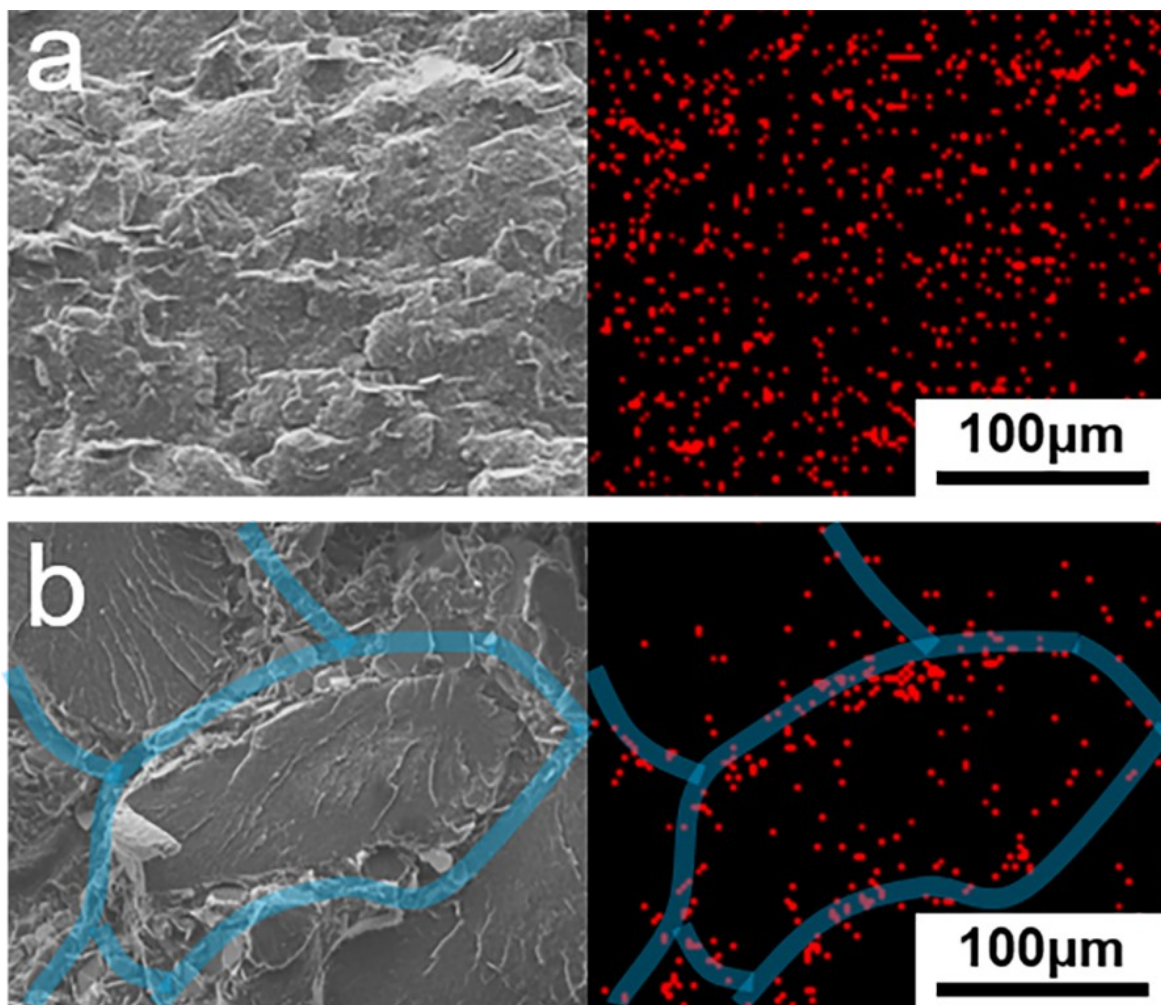


Fig. S6. SEM and EDS images of (a) r-8B8C and (b) s-8B8C.

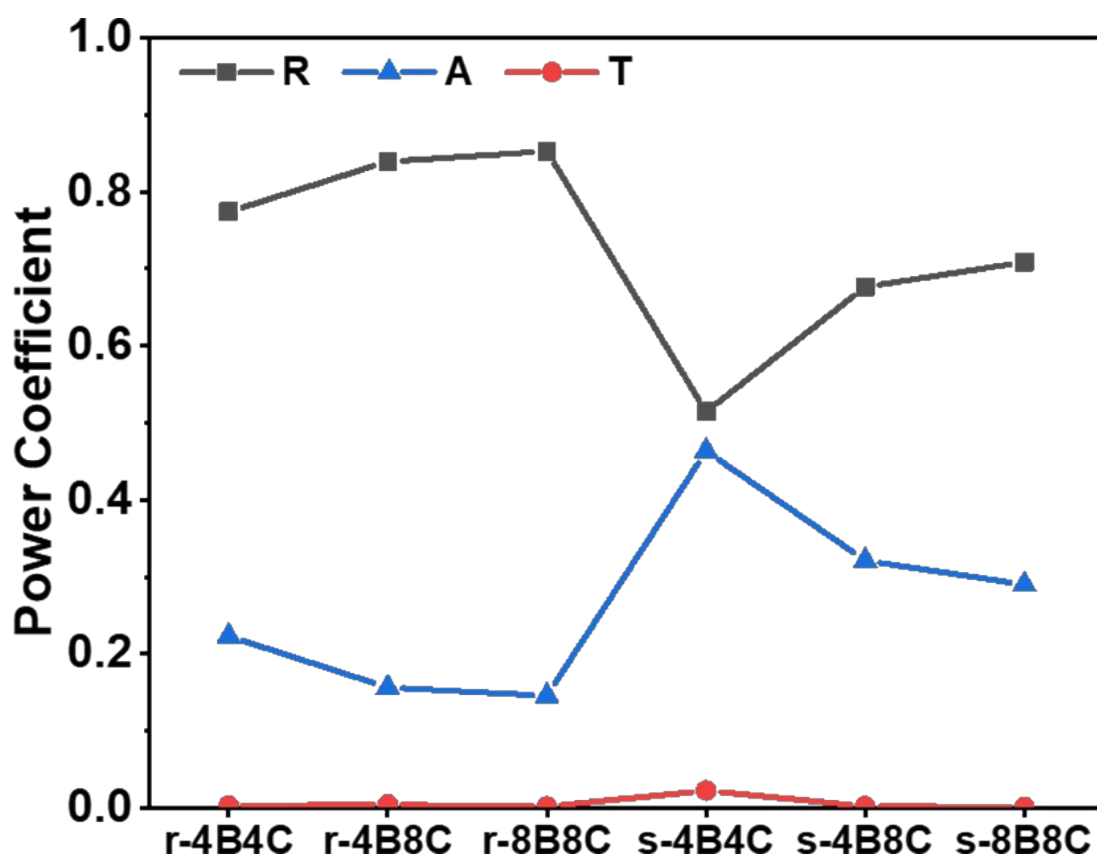


Fig. S7. Reflection (R), absorption (A), and transmission (T) coefficients of various materials.

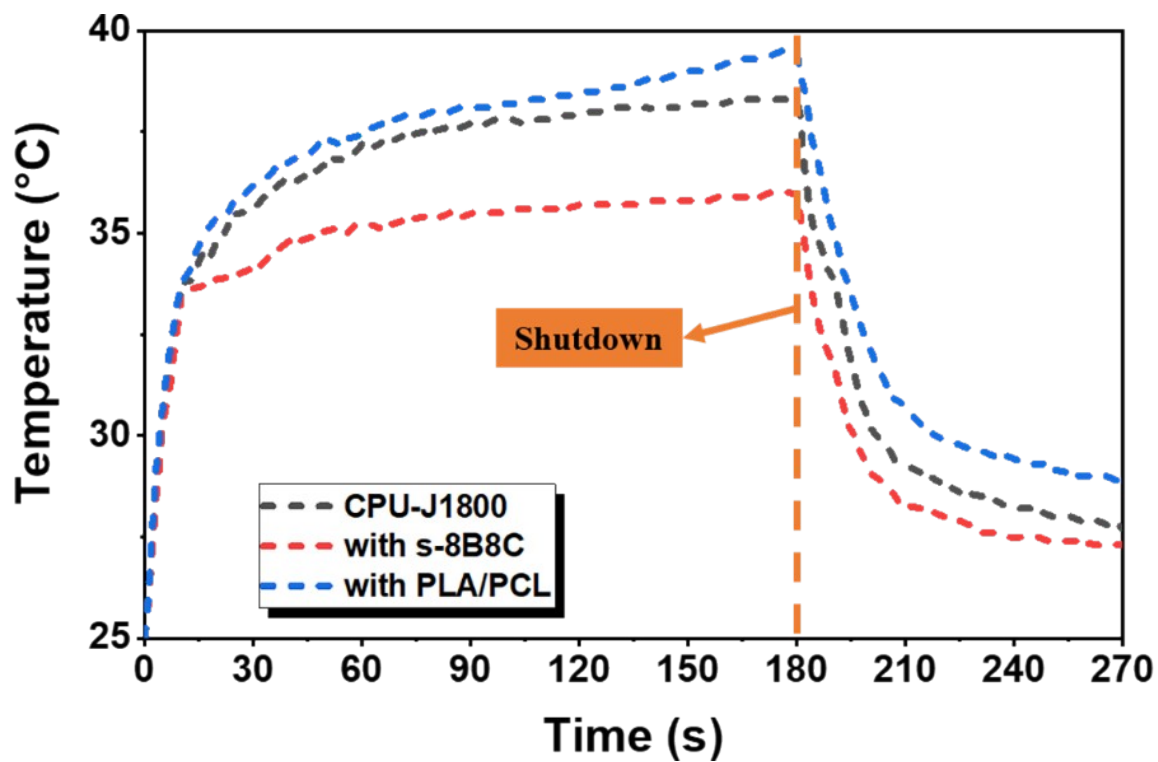


Fig. S8. Thermal performance test of the CPU-J1800.

Table S1. Electrical conductivity and volume resistivity of various samples.

Sample	PLA/PCL	r-4B4C	r-4B8C	r-8B8C	s-4B4C	s-4B8C	s-8B8C
Electrical conductivity (S/m)	4.3×10^{-14}	41.7	116.3	128.2	3.7×10^{-12}	2.6×10^{-11}	1.4×10^{-10}
Volume resistivity ($\Omega \cdot \text{cm}$)	2.3×10^{15}	2.4	0.9	0.8	2.7×10^{13}	3.9×10^{12}	7.2×10^{11}

Table S2. Thermal conductivity (TC) of various samples.

Sample	PLA/PCL	r-4B4C	r-4B8C	r-8B8C	s-4B4C	s-4B8C	s-8B8C
TC(W/m·K)	0.15	0.31	0.37	0.42	0.29	0.39	0.60

References

- [1] Wang J, Song T, Ming W, Yele M, Chen L, Zhang H, et al. High MXene loading, nacre-inspired MXene/ANF electromagnetic interference shielding composite films with ultralong strain-to-failure and excellent Joule heating performance [J]. *Nano Research*. 2023;17(3):2061-2069.